# Geometrical technique to determine the influence of monochromatic aberrations on retinoscopy

**Austin Roorda**

*School of Optometry and Department of Physics, Guelph-Waterloo Program for
Graduate Work in Physics, University of Waterloo, Waterloo, Ontario N2L 3G1, Canada*

**William R. Bobier**

*School of Optometry, University of Waterloo, Waterloo, Ontario N2L 3G1, Canada*

A geometrical-optical analysis is developed to predict the reflex observed in retinoscopy. The analysis can be expanded to explain the reflex for an eye with aberrations. The succession of reflexes across the pupil for each position of the retinoscope is represented in a contour plot. The plots demonstrate that retinoscopy can be considered a measure of the transverse ray aberration of the eye. For an eye with simple defocus this causes the typical with and against motions observed with hyperopic and myopic refractive errors. For an eye with aberrations we predict more-complex retinoscopic reflexes. This theory is confirmed by actual measurements on a human eye with known aberrations.

*Key words:* retinoscopy, monochromatic aberrations, vision, eccentric photorefraction, refraction. © 1996 Optical Society of America

## 1. INTRODUCTION

Retinoscopy is well past its centenary as a standard clinical procedure to measure objectively the refractive state of the eye.[1] Retinoscopy is a double-pass technique in which light from a retinoscope is imaged onto the retina and is then reflected back to the retinoscope. The retinoscopist viewing through the sight hole in the retinoscope typically observes a change in the pattern of light in the subject's pupil as the beam is driven across it. The apparent movement is in the same direction as the movement of the retinoscope (termed "with" motion) when the eye is focused behind the retinoscope and in the opposite direction (termed "against" motion) when the eye is focused in front of the retinoscope.

Refractive error is measured by the retinoscopist's placing a series of ophthalmic trial lenses before the eye and nulling (neutralizing) the motion of the reflex. Neutralization occurs when the combined optical power of the eye and the lens places the retina conjugate with the retinoscope. In this case, if only defocus is present, the reflex is rapid and has no direction.

Optical aberrations of the eye, however, will influence the retinoscopic measure, making the point of neutrality less precise. Chromatic aberration causes multiple focal planes at different wavelengths. Thus, near neutrality, both with and against motions are observed for different wavelengths. By filtering the wavelengths returning to the eye of the retinoscopist, the reliability of retinoscopy can be improved.[2]

Monochromatic aberrations of the eye produce more-complex effects, which cannot be easily removed.[3] Students of retinoscopy have been taught to pay attention to the reflex in the center 3−4 mm of the pupil and disregard reflexes arising from the periphery, especially when the pupil is dilated by cycloplegic agents.[3−6]

Retinoscopy has been used to measure the degree of aberration in the human eye. Jackson[7] used retinoscopy to measure the symmetrical aberration in the eye. Tscherning,[8] Brudzewski,[9] Pi,[10] Stine,[11] and Jenkins[12] used retinoscopy to determine the degree of aberration by measuring refraction in separate zones of the human eye.

### A. Previous Optical Analyses of Retinoscopy

According to a historical review by Jackson,[6] Bowman,[13] in 1859, was the first to refer to the observation of a light reflex in the pupil observed with the ophthalmoscope. At that time retinoscopy was used only to diagnose the presence of astigmatism and irregular refraction of the eye. Cuignet[14] developed it in 1873 as a technique to measure and correct for refractive errors in the eye, and since then it has evolved and become one of the standard clinical techniques used today. Previously published optical descriptions of retinoscopy typically provide only a simplified analysis of the origin of with and against motion in the defocused eye.[5,15] Swaine[16−19] used a model to predict the intensity of the reflex in the presence of defocus. Most references state that aberrations tend to alter the expected patterns, but, to our knowledge, none, with the exception of Hodd,[20] has predicted the effects of aberrations on the intensity profiles of the retinoscopic reflex.

Hodd expanded on the model used by Swaine to determine the intensity of the retinoscopic reflex of an eye having defocus. To determine the effects of aberrations he separated the pupil into annular zones, each having a different power. He determined the reflex in each zone independently and added the reflexes together to yield the total predicted reflex. His analysis did not consider the contribution of light entering one zone that is diffusely reflected from the retina and contributes to the reflex in the other zones. Despite this simplification, our results show similar features to those of Hodd.

### B.  Current Optical Analysis

The light reflex in retinoscopy arises from a source that is varying in its eccentricity from the sight hole during the sweep of the retinoscope. This analysis provides a detailed prediction of the pupillary light reflex for sequential positions of the retinoscope and allows us to model the monochromatic aberrations of the eye. If the aberrations are known, we can predict what the retinoscopic reflex will be.

Our technique uses computer algorithms to trace many rays through the eye. We used this technique to predict successfully intensity profiles in eccentric photorefraction for any degree of aberration.[21,22] Previously we modeled the optics of eccentric photorefraction, using a source whose position was fixed with respect to the camera aperture.[23,24] The camera aperture was assumed to be large. In adapting the model to analyze the optics of retinoscopy, two major changes had to be made. First, we allowed for the motion of the source with respect to the sight hole induced by tilting the retinoscope, and second, we had to consider the finite limits of the small sight-hole aperture. Furthermore, the retinoscopist typically uses corrective lenses to neutralize the reflex, whereas eccentric photorefraction is more rapid by allowing for image analysis of a single pupillary light reflex, although the use of corrective ophthalmic lenses is possible.[25,26] The unique feature of our model is that it explicitly considers the double-pass nature of the formation of the reflex and it can be used for any general aberration in the eye. The analysis is performed in two steps, the first for light entering the eye and the second for light leaving the eye. Because, in most cases, retinoscopy is performed along the principal astigmatic meridians, our analysis is limited to measurements along these meridians.

In our current study, our optical model is tested empirically. We investigate the possibility of determining the transverse aberration of the eye by using a hand-held retinoscope and also use a CCD-based retinoscope to provide a more quantitative comparison of the experimental and predicted results.

## 2.  THEORY

A standard retinoscope has a source located in the handle of the instrument. The light from the source reflects from a mirror oriented 45° from vertical, forming a virtual image of the source behind the mirror. The retinoscopist views the pupil of the subject through a small sight hole in the center of the mirror. The retinoscopist directs the divergent beam from the virtual source toward the subject's pupil and drives it across the pupil by tilting the retinoscope. Hereafter we refer to the driving of the beam as scoping. Tilting the retinoscope causes the virtual image of the light source to shift its eccentricity from the sight hole in the center of the mirror (Fig. 1). The changing eccentricity of the source with respect to the sight hole causes the appearance of the reflex to change, depending on the refractive state and aberrations in the eye.

### A.  Simplified Model

The retinoscopist uses motion and brightness of the reflex to determine the refractive state of the eye. We present a simplified model that will qualitatively explain the phenomenon of reflex motion. This model illustrates how the presence of defocus and aberrations affect the waist of rays returning to the retinoscope and predicts the resulting retinoscopic reflexes (Fig. 2). As shown in Fig. 1, one normally tilts the retinoscope and causes a movement of the virtual source of light with respect to the aperture. To simplify the ray diagrams in Fig. 2, we use a frame of reference in which the sight-hole aperture moves with respect to the source as the retinoscope is tilted. The simplified model considers only the second pass through the optics. We assume that there is a small spot projected onto the retina that diffusely reflects, thereby acting as a secondary source of light. The light from the spot on the retina emerges from the subject's pupil into a fan of rays whose intercepts are determined by the defocus and aberration of the eye. The principle of the origin of the reflex is that, if a ray from a particular point in the subject's pupil enters the sight-hole aperture, then that point on the pupil will appear luminous. One observes the succession of reflexes by moving the aperture across the fan of rays that emerges from the subject's pupil.

The simplified model offers a quick and intuitive explanation for the origin of the reflex based on the waist of rays at the retinoscope and the relative change in source-aperture eccentricity. This model is easy to visualize and is usually sufficient to explain effects of defocus and aberrations in retinoscopy because the retinoscopist generally concentrates on the motion of the retinoscopic reflex. For a complete description, however, we must consider the extended blur on the retina from the first pass through the optics.

### B.  Analysis of Monochromatic Aberrations

The ray tracing model uses the same theory that was previously used to predict eccentric photorefractive intensity profiles.[22] In our analysis the eye is modeled as a single refracting surface, where the function $k(\mathbf{r})$ defines the aberrations in the eye. This function repre-
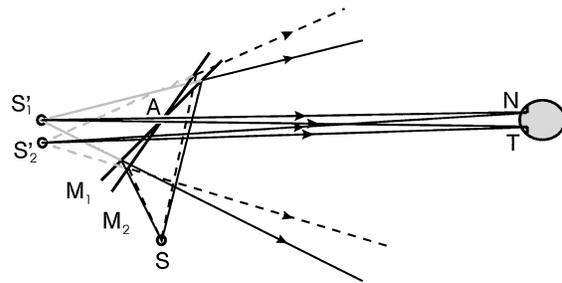


Fig. 1. Changes in eccentricity of the virtual source in retinoscopy. A virtual image (S′) is formed in reflection of actual source S located in the handle of the retinoscope by a silvered mirror (shown in two orientations, $M_1$ and $M_2$). When the direction of the retinoscope beam is changed (by tilting the mirror $M_1$ to $M_2$) the virtual source position will change in a direction opposite to the direction of the beam ($S_1'$ to $S_2'$). Thus, if the retinoscopist scopes across the eye in a temporal (T) to nasal (N) direction, the virtual image of the source will move in the opposite direction. The light patterns seen in retinoscopy can be attributed to the dynamic changes in the eccentricity of the virtual source with respect to the sight-hole aperture of the retinoscope (A). The optics of retinoscopy is therefore similar to eccentric photorefraction (adapted from Roorda et al.[27]).
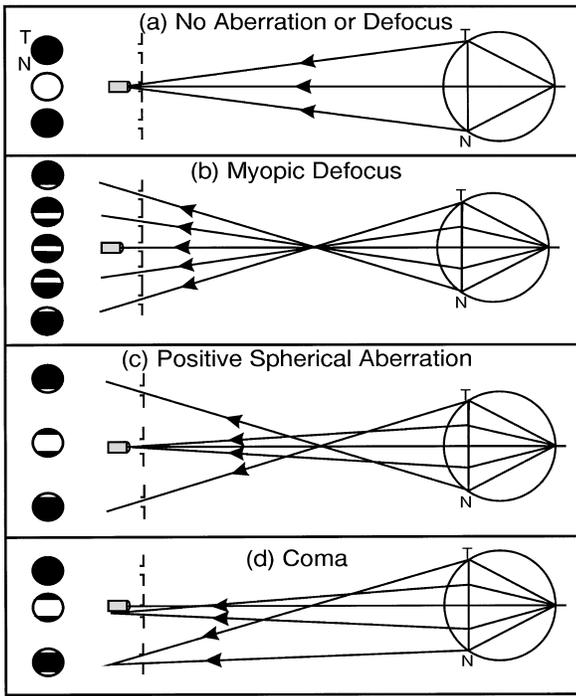
Fig. 2. Each figure illustrates a fan of rays emerging from a point source on the retina. The circles at the left in each figure represent the succession of reflexes that would appear in the pupil as the retinoscopist scopes from the temporal (T) to the nasal (N) side of the pupil. The sweep of the retinoscope is represented in this case by a series of eccentric apertures (sight holes) passing before a fixed source. Moving from top to bottom represents the case in which the source is offset nasally through to a temporal offset, which is achieved by scoping from the temporal to the nasal pupil margin. (a) For the aberration-free eye focused at the retinoscope, all the light returning from the retina focuses to a point. When the sight hole is at this point, light from all the rays across the pupil enter the aperture, and the pupil appears fully illuminated. While scoping in either direction, at first no reflex is observed and then the retinoscopist observes a rapid appearance of light with no directional movement. (b) With myopic defocus, the rays from the retina focus in front of the retinoscope. Scoping from the temporal to the nasal side of the pupil results in a reflex that moves from the nasal to temporal side (i.e., against motion). (c) With positive spherical aberration, the marginal rays focus earlier than the paraxial rays. When the beam is directed at the temporal pupil, first a narrow reflex appears at the nasal margin, followed by a wide reflex from the more paraxial rays. (d) With coma, rays from the margin focus off axis, and so reflexes from both edges of the pupil will appear simultaneously. When the aperture is on axis the paraxial region is well corrected. When the retinoscope is swept temporal to nasal, the retinoscopist observes a reflex that begins as a central broad band and separates into two reflexes at the margins (adapted from Roorda et al.[27]).

sents the change in the far point of the eye as a function of the radius from the geometrical center of the pupil (Fig. 3). In other words, $k(\mathbf{r})$ defines the distance to the intersection point of a ray emerging at radius $\mathbf{r}$ with the principal ray ($\mathbf{r} = 0$). This function can be derived from measurements that use either objective[28,29] or psychophysical[30,31] techniques. The function $k(\mathbf{r})$ can define both symmetric (e.g., spherical) and asymmetric (e.g., coma) aberrations. A constant value of $k$ represents a simple defocus error for which the far point is the same for all radii. The refractive state of the eye is the reciprocal of this value; $K = 1/k$. By conven-

tion, for distances measured perpendicular to the optical axis, temporal is positive and nasal is negative. Also, $k(\mathbf{r})$ is negative for distances measured in front of the eye and positive for distances measured behind the eye. The aberration commonly measured experimentally is the transverse aberration. The transverse aberration, $t(\mathbf{r})$, is a measure of the general ray intercept position from the principal ray intercept in a plane perpendicular to the optical axis. The conversion from $t(\mathbf{r})$ to $k(\mathbf{r})$ can be calculated by geometrical optics and is given by

$$k(\mathbf{r}) = \frac{l}{\left[1 - \frac{t(\mathbf{r})}{\mathbf{r}}\right]}, \qquad (1)$$

where $l$ (negative in front of the eye, positive behind the eye) is the distance to the plane where $t(\mathbf{r})$ is measured.

In the first step of the analysis we indirectly determine the blur on the retina from the retinoscope source. Rays are not explicitly traced into the eye. Instead, the principal rays emerging from the blur on the retina are determined. This is done by the following procedure. A single ray from the source enters the pupil, strikes the retina, and diffusely reflects. Using the principle of reversibility of optical rays, one can trace one of the diffusely reflected rays back along the path of the incoming ray. This ray must intersect the principal ray that originates from the same point on the retina. By induction, we can draw the principal ray to intersect the incoming ray at the far point for the particular radius at which the beam enters the entrance pupil of the eye (Fig. 4). We then find the intersection point of the principal ray in the retinoscope plane by extending the ray to the plane of the retinoscope. In this analysis, no rays need to be traced
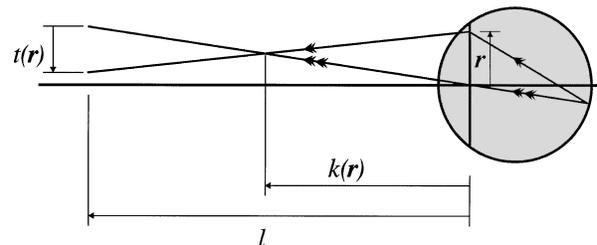


Fig. 3. A ray (single arrow) emerging from a retinal point passing through the exit pupil at a radius $\mathbf{r}$ crosses the principal ray (double arrows) from the same point a distance $k(\mathbf{r})$. The transverse aberration, $t(\mathbf{r})$, is a measure of the emerging ray intercept position from the principal ray intercept in a plane perpendicular to the optical axis at a specified distance $l$ from the exit pupil.
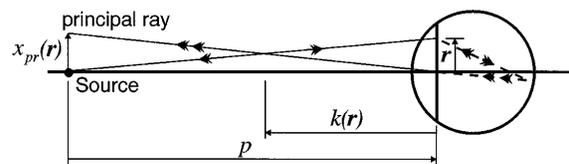


Fig. 4. Determining the principal ray. The dashed rays inside the eye are not necessary for determining the position of the principal ray and are used only to clarify the illustration. The principal ray is drawn from the center of the exit pupil and intersects the incoming ray at the specific far point $k(\mathbf{r})$ for the radius $\mathbf{r}$ at which the ray enters the eye.
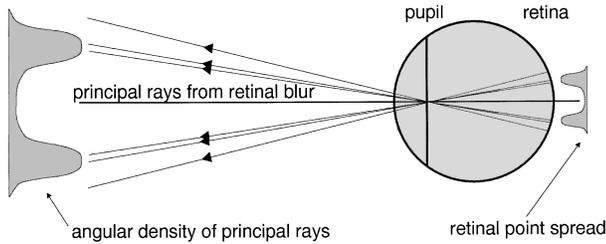
Fig. 5.   Principal rays emerging from the blur on the retina. In the first step of the analysis we determine the principal ray emerging from each point on the retinal blur.   This construction shows that the angular density of principal rays is a scaled equivalent of the blur on the retina (from Roorda *et al.*[22]).

into the eye; thus the exact optics of the eye need not be known.   The intersection of the principal ray with the retinoscope plane is calculated by[21]

$$x_{\mathrm{pr}}(\mathbf{r}) = \mathbf{r} \frac{[p + k(\mathbf{r})]}{-k(\mathbf{r})}, \tag{2}$$

where $x_{\mathrm{pr}}(\mathbf{r})$ is the distance from the source to the intersection of the principal ray in the retinoscope plane (in millimeters), $\mathbf{r}$ is the ray position in the pupil (millimeters), $p$ is the retinoscope distance (meters), and $k(\mathbf{r})$ is the far-point position as a function of the radius (meters).

The procedure is repeated for each ray that enters the eye.   The result is a distribution of principal rays emerging from the blur on the retina.   The angular density of principal rays is a scaled equivalent to the intensity of the retinal point spread (Fig. 5).

Each point across the blur on the retina reflects diffusely.   Each diffusely reflected ray intersects its principal ray at a distance determined by the far point for the radius at which it leaves the eye (Fig. 6).   The position where each diffusely reflected ray from a particular point on the retina intersects the retinoscope plane is calculated by[21]

$$y(\mathbf{r}) = x_{\mathrm{pr}} + \mathbf{r} \frac{[p + k(\mathbf{r})]}{-k(\mathbf{r})}, \tag{3}$$

where $y(\mathbf{r})$ is the distance from the source to the intersection of the returning ray (millimeters) and $x_{\mathrm{pr}}$ is the distance from the source to the intersection of the principal ray with the retinoscope plane (millimeters) as defined in Eq. (2).

In Subsection 2.A it was stated that, if a ray from a particular point in the subject's pupil enters the sight-hole aperture, then that point on the pupil will appear luminous.   Therefore we can conclude from Eq. (3) that the reflex will appear in the pupil at the positions $\mathbf{r}$ for which $y(\mathbf{r})$ lies within the bounds of the sight-hole aperture.   This is given mathematically by

$$e - (a/2) \leq y(\mathbf{r}) \leq e + (a/2), \tag{4}$$

where $e$ is the source eccentricity from the center of the sight-hole aperture and $a$ is the width of the sight-hole aperture.   It is possible for there to be more than one reflex originating from a single point on the retina if aberrations are present in the eye.

Each point across the blur on the retina may produce a reflex.   The intensity of each reflex is proportional to

the intensity of the point on the retina that produces it. All the reflexes are added together to produce the full retinoscopic reflex for a single source position.   Repeating the procedure for a range of source positions generates the succession of reflexes that one observes while scoping once across the pupil.   Figure 7 shows the reflex for a range of source positions.   Each graph represents the succession of reflexes that would appear while one scopes once across the pupil.   We chose to graph the results in this manner to illustrate that retinoscopy is a measure of the transverse ray aberration in the eye.   Note the similarity between the transverse aberration plot and the contour map of the succession of reflexes.

## C.   Computer Program
A computer program was used to perform the iterative ray tracing and produce the intensity profiles.   Each intensity profile required less than 1 min with a BASIC program running on a 486 PC.   The time depended on the sensitivity selected.   In our simulations, rays were traced into the eye and the source position was varied at 0.2-mm intervals.   The program output an array of intensity as a function of pupil position versus source position.

## 3.   EXPERIMENT

### A.   Aberration Measurement
The measurement of monochromatic aberrations across the horizontal meridian in the eyes of the subjects was made with a previously developed modified Ivanoff apparatus.[30]   The method permits a psychophysical determination of the transverse ray aberration through a horizontal alignment of a vertical vernier seen in normal view with a similar vernier seen in Maxwellian view. Traversing the Maxwellian view across the pupil and measuring the resulting displacement of the vernier targets define the ray aberration for each subject.   A polynomial was fitted to the transverse aberration data for each subject by SAS System software version 6.07.01 on a Unix-based system to produce a smooth aberration function.

The fitting procedure is a backward fitting of a fifth-order polynomial.   Coefficients with less than 95% confi-
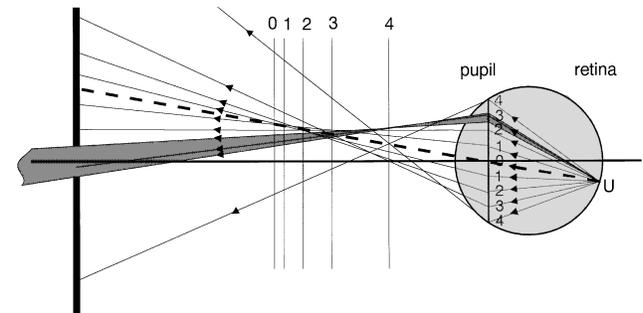


Fig. 6.   The shaded region represents the bundle of rays that enter the sight-hole aperture.   In this figure we have modeled a myopic eye with positive spherical aberration.   The rays from point U on the retina cause illumination of the region from 2.5 to 3.1 mm on the pupil.   The illumination distribution across the pupil is calculated for each point across the retinal point spread, and the distributions are summed together to yield the retinoscopic reflex for a single source position.
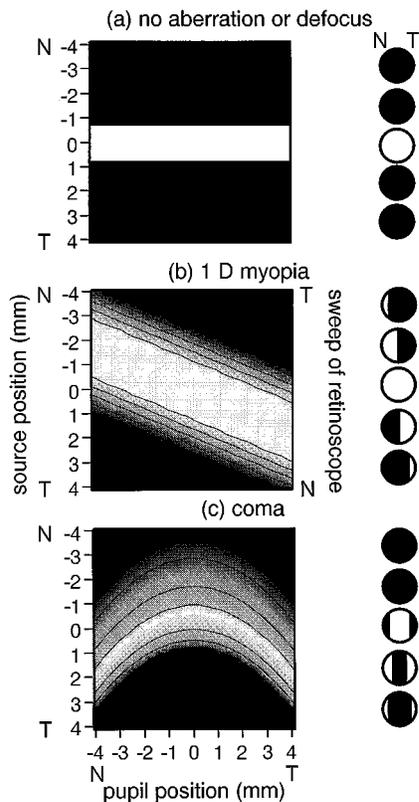
Fig. 7. Each figure represents the intensity distribution across the pupil for each position of the source with respect to the sight-hole aperture. Position zero on the source position scale represents the center of the 1.5-mm sight-hole aperture. The succession of intensity profiles at each source position simulates the motion of the reflex observed in retinoscopy. Sweeping the retinoscope temporal (T) to nasal (N) corresponds to a nasal-to-temporal movement of the source. The circles on the right of the plots are similar to those used in Fig. 2 and provide an aid for visualizing the changing reflex as it would appear in the pupil. In (b) and (c) the maximum intensity represents the relative intensity compared with the zero-aberration case. (a) No aberration: when the source position coincides with the sight hole, the reflex fills the pupil and does not vary while the source position lies within the bounds of the aperture. Once the source position lies eccentric to the sight hole, the pupil appears dark. (b) Myopic eye, 0.75-D defocus: the maximum intensity of the reflex is lower, and the reflex crosses the pupil in an against motion. While the source is within the bounds of the aperture the pupil appears fully illuminated but not even in intensity. (C) Coma: in this case the reflex begins in the center of the pupil and separates to form a split reflex at each margin.

dence are discarded from the fit. The function fit is

$$t(\mathbf{r}) = A_1\mathbf{r}^3 + A_2\mathbf{r}^5 + B_1\mathbf{r}^2 + B_2\mathbf{r}^4 + C\mathbf{r} + \Delta t, \quad (5)$$

where $A_1$ and $A_2$ are coefficients of third- and fifth-order spherical aberration, respectively, $B_1$ and $B_2$ are coefficients of third- and fifth-order coma, respectively, $C$ is the defocus coefficient, and $\Delta t$ is the zero offset term. Equation (1) is applied to convert $t(\mathbf{r})$ to longitudinal aberration.

## B. Subjective Retinoscopy

To test whether the transverse aberration could be observed with the standard hand-held streak retinoscope, the retinoscopist sketched the succession of reflexes that appeared in the pupil after the best paraxial correc-

tion was achieved with trial lenses. The retinoscopist sketched the edges of the reflex across the horizontal meridian but did not determine the intensity profile. For each subject, AR and IB, a series of seven sketches was obtained that represented a single sweep of the retinoscope.

## C. Simulated Retinoscopy

We simulated a retinoscope by using the apparatus illustrated in Fig. 8 with a sight-hole width of 1.5 mm, a source width of 1.5 mm, a subject-to-sight-hole distance of 0.42 m, and a subject-to-source distance of 0.475 m. The images were captured with a Canon Ci-20R infrared CCD camera with a computer interface.

We simulated a slit source by placing a slit aperture in front of two infrared LED's adjacent and oriented perpendicular to the direction of motion of the source. The LED's radiated at approximately 950 nm (FWHM 100 nm). The allowable exposure limit according to published standards is 1012 $\mu$W/cm$^2$ for continuous exposure.[32] The total power of the two LED's was less than half of this level. We made a sight hole in a mirror by removing a 1.5-mm-wide section of reflective backing from a silvered mirror. As a consequence, when the source was coincident with the sight hole, less of the beam reflected to the eye, thereby reducing the intensity of the reflex.

We captured a series of pupil images with both temporal and nasal source positions at 0.5-mm intervals. By means of an ophthalmic trial lens, the paraxial focus was set to coincide with the aperture plane. We determined the power of the ophthalmic lens by traversing the source across the sight hole and selecting the lens that neutralized the reflex motion in central pupillary area.

Two retinoscopic measurements were performed on subject AR. The subject's eye was dilated with a single drop of 1% cyclopentolate. In the first experiment we performed retinoscopy on the unaided eye.

We repeated the procedure with the same eye fitted with a soft varifocal contact lens (PA1, Bausch & Lomb, nominal power +0.75 D). This lens had varying focal lengths across its surface that induced a large degree of aberration in the eye. In spite of these aberrations, the subject still had a best-correction visual acuity of 20/15. In both cases we ensured that the eye was paraxially focused on the sight-hole aperture before obtaining a series of images. No significant degree of astigmatism
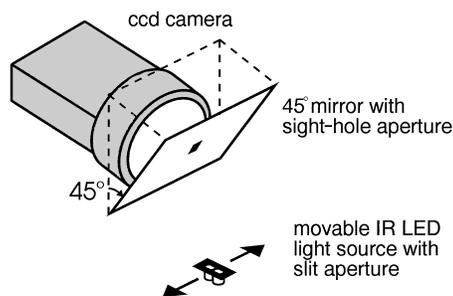


Fig. 8. Apparatus for CCD streak retinoscopy. The light source is composed of two adjacent infrared LED's set behind a slit aperture. The mirror is fully reflecting, except for a transparent sight hole 1.5 mm wide in the center. A micrometer stage is used to vary the source position with respect to the sight hole. The CCD focuses through the sight hole onto the pupil of the subject.
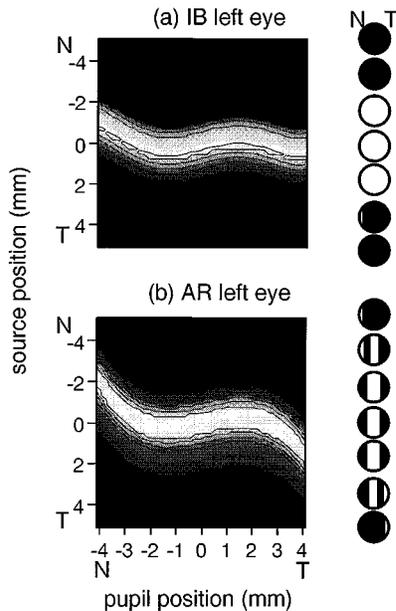
**Fig. 9.** Each figure represents the intensity distribution across the pupil for each position of the source with respect to the sight-hole aperture. Position zero on the source position scale represents the center of the 1.5-mm sight-hole aperture. The succession of intensity profiles for a range of source positions simulates the motion of the reflex observed in retinoscopy. (a) Subject IB, left eye: IB has irregular aberrations, but they are very low across the entire dilated pupil. (b) Subject AR, left eye: AR has primarily third-order spherical aberration along the horizontal meridian with some defocus. The circles on the right side of each figure are the retinoscopist's sketches of the reflexes observed in the subject during retinoscopy scoping temporal (T) to nasal (N) (i.e., source position nasal to temporal). The crest of each of the graphs above traces the ray intercept function for each subject.

($<$ 0.25 D) was found in the eye with or without the contact lens. A single subject was used so that only the ocular aberrations were changed between the two trials while other intersubject variations, such as retinal reflectivity, were not.

## 4. RESULTS

### A. Retinoscopic Sketches

The succession of sketches gave us a good indication of the motion of the reflex. We compared the retinoscopic results with retinoscopic predictions for two subjects (Fig. 9). These results suggested that transverse aberration in the human eye is detectable with a standard hand-held retinoscope. We did not expect to determine the exact scale of the transverse aberration in the eye, but relative degrees of aberration were easily seen in practice with the retinoscope. The retinoscopist found very little reflex motion in the subject with low aberrations [Fig. 9(a)]. However, the retinoscopic sketches differed when greater degrees of aberration were present [Fig. 9(b)]. For both subjects neutrality was observed in the center of the pupil, but with the specific aberrations for the horizontal meridian of subject AR the succession of light patterns showed an against motion at the pupil margins.

One may notice that the retinoscopic prediction for the subject AR in Fig. 9(b) differs from that in Fig. 11(a).

The reason is that a defocus term (linear) is present in the simulation in Fig. 9(b). The defocus term was used in the simulation in Fig. 9(b) to compensate for a slight miscorrection of the paraxial region of the pupil.

### B. Simulated Retinoscopy

Figure 10 shows the transverse aberration measured for subject AR unaided and with the PA1 contact lens in place. Each curve is represented by a polynomial function. Figure 11 shows contour plots of the expected retinoscopic patterns for a range of source positions. Figure 12 shows the experimental results for the same cases. The crests of the contour plots of these experimental results follow the transverse ray aberration of the eye. We can observe this qualitatively in Figs. 11 and 12. We investigated this further by fitting a function across the peaks of the contour plots. Noise in the plots prevented an accurate assessment of the transverse aberration but gave a qualitative estimation of the degree of aberration
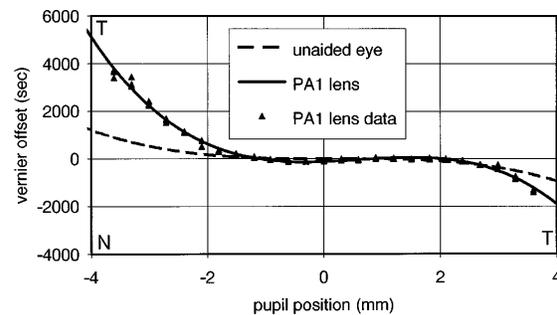


**Fig. 10.** Transverse ray aberration data for subject AR's left eye with and without the PA1 varifocal contact lens measured with the modified Ivanoff apparatus.[30] The unaided eye (dashed curve) has a nearly symmetrical aberration along the horizontal meridian. The PA1 lens induces a higher degree of aberration, particularly on the nasal edge. The symbols represent the actual data for the measurement of the transverse aberration. N, Nasal; T, temporal.
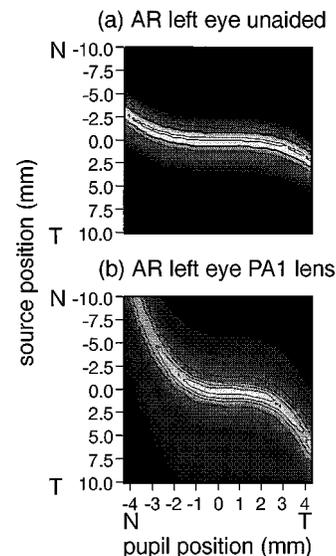


**Fig. 11.** Retinoscopic prediction for subject AR with and without the PA1 contact lens. The contour plots demonstrate that the retinoscopic predictions are measurements of the transverse ray aberration. Both contour plots are the retinoscopic predictions for the eye paraxially focused on the sight-hole aperture. N, Nasal; T, temporal.
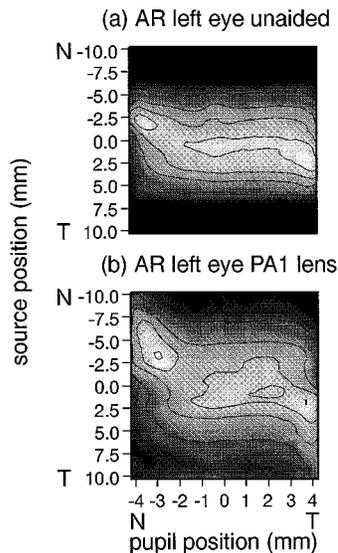
Fig. 12. Experimental retinoscopy results for subject AR with and without the PA1 contact lens. Each experimental profile across the horizontal meridian of the pupil is plotted in succession to form the contour plot. The results are similar to the predictions (Fig. 11). The central region of the pupil in each case shows no reflex motion. At the margins of the pupil the results from the unaided eye show the against motion of the reflex at the edges of the pupil, as we predicted. For the PA1 lens we found more of a reflex in the nasal (N) margin than in the temporal (T) margin, as was expected from the predictions.

in the eye. We determined the source position that produced an intensity peak for each pupil position and fitted a function to this series of points. The precision with which we could localize a peak was one source position interval (0.5 mm). A true test of the accuracy of the retinoscopic technique for measuring transverse aberration would be possible only if multiple measurements on a single eye were performed. Figure 13 shows plots of the data set and the function fit.

## 5. DISCUSSION

There are some discrepancies between our results and the theoretical predictions, which are due mainly to the simplifications of our model.

Our analysis is for aberrations and defocus along a single meridian. We make the assumption that a fan of rays entering the eye in a specific plane passes through the optics and exits the eye in the same plane, which is true only if the optical system is rotationally symmetric or the analysis is along a principal astigmatic and comatic meridian. Retinoscopic measurements performed along meridians other than the principal astigmatic or comatic meridians will show slight differences from the expected intensity profiles. In this study and in our previous paper,[22] intensity profiles were smoother than expected. Although there was no significant astigmatism in the subjects' eyes, we could not be certain that our measurements were made along the principal comatic meridian, which may have caused some of the discrepancy. However, in considering the agreement of our experimental with the predicted results, we conclude that most of the contribution to the intensity profile in retinoscopy and in photorefraction is due to aberrations and to defocus errors along the meridian in which the profile is measured.

The extent of source positions over which the pupillary reflex appeared in our experimental measurements was greater than predicted. We suggest two reasons for this: reflections originating from multiple surfaces in the retina[33,34,35] and the extended source of the retinoscope. To correct for multiple reflections one would have to sum results from several graphs with the defocus term and the relative intensity adjusted for each reflecting surface. One can model an extended source by adding each simulated profile with its neighboring profiles up to the width of the source, thereby performing a convolution of the contour plot with itself over the width of the source. Both of these corrections would cause smoothing of the predicted results.

The retina is not a perfectly diffuse reflector but produces directional reflections because of the waveguide nature of the photoreceptor array.[36] This directionality tends to reduce the intensity of the reflexes at the edge of the pupil. This effect of photoreceptor waveguiding was more difficult to observe experimentally because the intensity of the reflex was reduced when the source was in line with the sight-hole aperture (see Subsection 3.C).

## 6. RECOMMENDATIONS FOR RETINOSCOPY

When one is performing retinoscopy, ocular defocus will be the main cause of the reflex motion until the eye is near correction; then the effects of aberration will dominate.
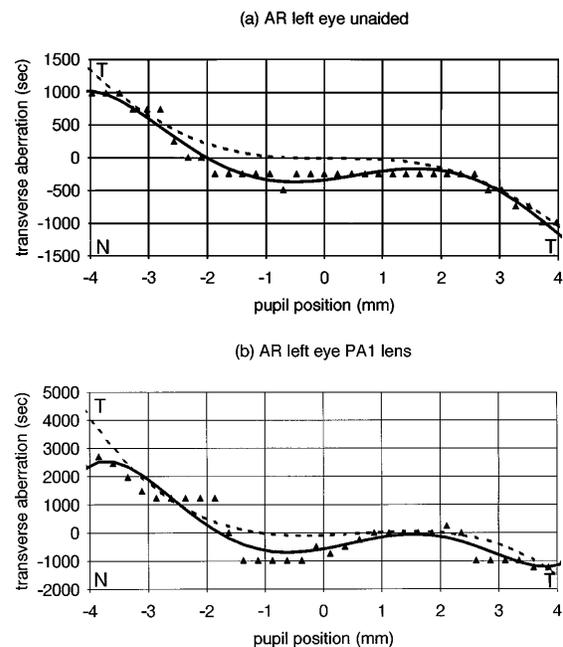


Fig. 13. Estimations of the transverse ray aberration in subject AR derived from experimental retinoscopic results. We determined the source position at the peak of each vertical profile of the contour plot (Fig. 12) and fitted a function of peak position versus pupil position. The plots are converted to represent the transverse ray intercept in seconds of arc. The solid curves are the best fits of fifth-order polynomial functions to the data. The dashed curves represent the transverse aberrations by the modified Ivanoff method (from Fig. 10). (a) Transverse aberration, subject AR, unaided eye: Correlation coefficients: for modified Ivanoff method $r^2 = 0.98$, for retinoscopy method $r^2 = 0.98$. (b) Transverse aberration PA1 contact lens. Correlation coefficients: for Ivanoff method $r^2 = 0.99$, for retinoscopy method $r^2 = 0.97$. T, Temporal; N, nasal.

After the best retinoscopic correction has been achieved, the reflex will not have any apparent motion over the central region of the pupil, and the motion of the reflex that persists will be in the periphery and is due to the aberrations of the eye. Therefore this study supports the clinical rule of thumb that advises the retinoscopist to neutralize the reflex in the center of the pupil. The main point is that one should perform retinoscopy on as much of the visual zone as possible. Considering the aberrations, one would get a reasonable reflex for subject AR if the pupil were as large as 5 mm. With PA1 lens in place the zone would be reduced to less than 4 mm. For subject IB the retinoscopist was confident in performing the refraction on the entire dilated pupil. The retinoscopist must therefore decide the size of the refracted zone based on the individual subject. To go automatically to a small pupil (3–4 mm) would not always be beneficial because of the increased depth of focus, the reduced intensity of the reflex, and the limited distance over which motion of the reflex can be determined. However, in some instances the small pupil may be necessary.

In the case of spherical aberration one may see against motion (positive spherical aberration) or with motion (negative spherical aberration) at the edges of the pupil. In the case of coma, one may observe a reflex that begins in the center of the pupil and splits to two bright reflexes at each margin. For combinations of these aberrations and for higher-order aberrations, more-complex reflexes will be seen. With this in mind, a retinoscopist could potentially detect and differentiate between comatic and spherical type aberrations in the eye by using retinoscopy. This motion cannot be corrected with a standard lens, so it should be ignored when one is performing a retinoscopic refraction, provided that a correction over the central region of the pupil has been achieved. The eye will compensate for aberrations at the edges of the pupil through the Stiles–Crawford effect, and, under most circumstances, the pupil is small enough that it will mask the regions of the optical system that are afflicted with these aberrations.

## 7. CONCLUSIONS

The reflexes observed in retinoscopy can be explained through consideration of a virtual light source changing in its relative eccentricity and direction with respect to the instrument's sight-hole aperture. This optical analysis is quantitatively supported from empirical measures of light patterns in the pupil taken from a video-based simulation of retinoscopy and qualitatively supported by sketches from a standard streak retinoscope measurement. The monochromatic aberrations of the eye alter the retinoscopic reflex primarily at the edges of the pupil. Spherical and comatic aberrations cause the peripheral light reflex to linger beyond that of the central area during the sweep of the retinoscope. Retinoscopy will be most accurate when measurements are made in the central part of the pupil where aberrations are the smallest.

## ACKNOWLEDGMENTS

## REFERENCES

1. M. Millodot, " A centenary of retinoscopy," J. Am. Optom. Assoc. **44,** 1057–1059 (1973).
2. C. W. Bobier and J. G. Sivak, "Chromoretinoscopy and its instrumentation," Am. J. Optom. Physiol. Opt. **57,** 106–108 (1980).
3. G. Walsh, "Why a distorted ret reflex is normal," Optician (October 13, 1994), pp. 11–22.
4. P. H. O'Connor-Davies, *The Actions and Uses of Ophthalmic Drugs,* 2nd ed. (Butterworth, London, 1981).
5. J. I. Pascal, *Modern Retinoscopy* (Hatton, London, 1930).
6. E. Jackson, *Skiascopy and Its Practical Application to the Study of Refraction,* 4th ed. (Herrick, Denver, Colo., 1905).
7. E. Jackson, "Symmetrical aberrations of the eye," Trans. Am. Ophthalm. Soc. **5,** 141–149 (1988).
8. M. Tscherning, *Physiologic Optics,* 4th ed. (Keystone, Philadelphia, Pa., 1924).
9. K. Brudzewski, "Beitrag zur Dioptrik des Auges," Arch. Augenh. **40,** 296–333 (1900).
10. H. T. Pi, "Total peripheral aberration of the eye," Trans. Ophthalmol. Soc. UK **45,** 393–399 (1925).
11. G. H. Stine, "Variations in refraction of the visual and extravisual pupillary zones," Am. J. Ophthalmol. **13,** 101–112 (1930).
12. T. C. A. Jenkins, "Aberrations of the eye and their effects on vision: Part I," Br. J. Physiol. Opt. **20,** 59–91 (1963).
13. W. P. Bowman, "On conical cornea and its treatment by operation," Ophthalmic Hospital Reports J. R. London Ophthal. Hosp. **2,** 154–167 (1859–1860).
14. F. Cuignet, "Keratoscopie," Rec. Ophthalmol. **2,** 14–23 (1873).
15. E. Landolt, "Methods of determination of the refraction and accommodation of the eye," in *The Refraction and Accommodation of the Eye,* C. M. Culver, ed. (Pentland, Edinburgh, 1886).
16. W. Swaine, "Retinoscopy. I. General outline and symbols," Optician (April 1945), pp. 171–179.
17. W. Swaine, "Retinoscopy. II. Basic theoretical principles," Optician (June 1945), pp. 335–339.
18. W. Swaine, "Retinoscopy. III. Variation of illumination across the reflex," Optician (August 1945), pp. 35–40.
19. W. Swaine, "Retinoscopy. IV. Variation of the reflex brightness with refractive error and pupil diameter," Optician (August 1945), pp. 71–74.
20. F. A. B. Hodd, "Retinoscopy," in *Some Advances in Ophthalmic Optics,* Transactions of the London Refraction Hospital, Jubilee Congress, October, 1947 (Hatton, London, 1947), pp. 146–234.
21. M. C. W. Campbell, W. R. Bobier, and A. Roorda, "Effect of monochromatic aberrations on photorefractive patterns," J. Opt. Soc. Am. A **12,** 1637–1646 (1995).
22. A. Roorda, M. C. W. Campbell, and W. R. Bobier, "Geometrical theory to predict eccentric photorefraction intensity profiles in the human eye," J. Opt. Soc. Am. A **12,** 1647–1656 (1995).
23. W. R. Bobier and O. J. Braddick, "Eccentric photorefraction: optical analysis and empirical measures," Am. J. Optom. Physiol. Opt. **62,** 614–620 (1985).
24. H. C. Howland, "Optics of photoretinoscopy: results from ray tracing," Am. J. Optom. Physiol. Opt. **62,** 621–625 (1985).
25. W. R. Bobier, P. Schmitz, G. Strong, J. Knight, K. Widdersheim, and H. C. Howland, "Comparison of three photorefractive methods in a study of a developmentally handicapped population," Clin. Vision Sci. **7,** 225–235 (1992).

26. F. Schaeffel, L. Farkas, and H. C. Howland, "Infrared photoretinoscope," Appl. Opt. **26,** 1505–1509 (1987).

27. A. Roorda, W. R. Bobier, and C. Teske, "Retinoscopic patterns: explained by the optics of an eccentric source," in *Vision Science and Its Applications,* Vol. 1 of 1995 OSA Technical Digest Series (Optical Society of America, Washington, D.C., 1995), pp. 121–124.

28. J. Liang, B. Grimm, S. Goelz, and J. F. Bille, "Objective measurement of wave aberrations of the human eye with use of a Hartmann–Shack wave-front sensor," J. Opt. Soc. Am. A **11,** 1949–1957 (1994).

29. G. Walsh, W. N. Charman, and H. C. Howland, "Objective technique for the determination of monochromatic aberrations of the human eye," J. Opt. Soc. Am. A **1,** 987–992 (1984).

30. M. C. W. Campbell, E. M. Harrison, and P. Simonet, "Psychophysical measurement of the blur on the retina due to optical aberrations of the eye," Vision Res. **30,** 1587–1602 (1990).

31. H. C. Howland and B. Howland, "A subjective method for the measurement of monochromatic aberrations of the eye," J. Opt. Soc. Am. **11,** 1508–1518 (1977).

32. *American National Standard for the Safe Use of Lasers ANSI Z136.1-1993* (American National Standards Institute, New York, 1993).

33. M. Millodot, "Reflection from the fundus of the eye and its relevance to retinoscopy," Atti Fond. Giorgio Ronchi **27,** 31–50 (1972).

34. F. C. Delori and K. P. Pflibsen, "Spectral reflectance of the human ocular fundus," Appl. Opt. **28,** 1061–1077 (1989).

35. W. N. Charman, "Reflection of plane polarized light by the retina," Br. J. Physiol. Opt. **34,** 34–49 (1980).

36. G. J. van Blokland and D. van Norren, "Intensity and polarization of light reflected at small angles from the human fovea," Vision Res. **26,** 485–494 (1986).